

Impact of uranium (U) on the cellular glutathione pool and resultant consequences for the redox status of U

Katrin Viehweger · Gerhard Geipel ·
Gert Bernhard

Received: 1 April 2011 / Accepted: 28 June 2011 / Published online: 14 July 2011
© Springer Science+Business Media, LLC. 2011

Abstract Uranium (U) as a redox-active heavy metal can cause various redox imbalances in plant cells. Measurements of the cellular glutathione/glutathione disulfide (GSH/GSSG) by HPLC after cellular U contact revealed an interference with this essential redox couple. The GSH content remained unaffected by 10 μM U whereas the GSSG level immediately increased. In contrast, higher U concentrations (50 μM) drastically raised both forms. Using the Nernst equation, it was possible to calculate the half-cell reduction potential of 2GSH/GSSG. In case of lower U contents the cellular redox environment shifted towards more oxidizing conditions whereas the opposite effect was obtained by higher U contents. This indicates that U contact causes a consumption of reduced redox equivalents. Artificial depletion of GSH by chlorodinitrobenzene and measuring the cellular reducing capacity by tetrazolium salt reduction underlined the strong requirement of reduced redox equivalents. An additional element of cellular U detoxification mechanisms is the complex formation between the heavy metal and carboxylic functionalities of GSH. Because two GSH molecules catalyze electron transfers each with one electron forming a dimer (GSSG) two UO_2^{2+} are reduced to

each UO_2^+ by unbound redox sensitive sulfhydryl moieties. UO_2^+ subsequently disproportionates to UO_2^{2+} and U^{4+} . This explains that in vitro experiments revealed a reduction to U(IV) of only around 33% of initial U(VI). Cellular U(IV) was transiently detected with the highest level after 2 h of U contact. Hence, it can be proposed that these reducing processes are an important element of defense reactions induced by this heavy metal.

Keywords Uranium · GSH/GSSG · Half-cell reduction potential · Redox process · Complex formation

Introduction

Uranium (U), a widespread naturally occurring radioactive heavy metal, causes several ecological problems due to increased anthropogenic dumping in the upper earth crust. Thereby its chemical toxicity as heavy metal plays a pivotal role in different ecosystems. Although U is a non essential metal it is taken up by plants and can therefore induce complex defence reactions or impair physiological functions (Günther et al. 2003; Viehweger and Geipel 2010).

A key element for maintenance of cellular redox balance is the tripeptide glutathione (GSH, reduced form; GS-SG, oxidised form) operating as a thiol/disulphide redox buffer (GSH/GS-SG) (Noctor and Foyer 1998; Foyer and Noctor 2005; Sharma and

K. Viehweger (✉) · G. Geipel · G. Bernhard
Biogeochemistry Division, Institute of Radiochemistry,
Helmholtz-Zentrum Dresden-Rossendorf eV,
P.O. Box 510119, 01314 Dresden, Germany
e-mail: k.viehweger@hzdr.de

Dietz 2009). Glutathione is temporary or sustained consumed by several reactions. These include protein S-glutathionylation, phytochelatin synthesis and detoxification of xenobiotics via conjugation catalysed by glutathione-S-transferase. In addition to the metal chelating phytochelatin, GSH is also able to form complexes with metals for example with U (Canovas et al. 2004; Singh 2005; Frost et al. 2011).

U could enable redox reactions in the cell because it is a redox active transition metal. These reactions might result in the formation of reactive oxygen species (ROS) via Fenton-type reactions. Consequently, exposure to U could be associated with changes in the cellular redox status. Recent studies in beans (*Phaseolus vulgaris*) and *Arabidopsis thaliana* suggested oxidative reactions caused by U indicated by altered levels of the glutathione pool and increased capacities of antioxidative enzymes like peroxidases (Vandenhove et al. 2006; Vanhoudt et al. 2008).

Thus, the aim of the present study was to investigate the impact of the redox active U on the cellular redox balance in canola cells (*Brassica napus*). The redox environment was characterised by determinations of the crucial redox couple 2GSH/GSSG and the resultant half-cell reduction potential. Due to the strong reducing capacity of GSH, its ability of reduction of U(VI)–U(IV) was investigated in vitro. Using the obtained results, the fate of U in the cytoplasm for instance the probability of a complex formation between the metal and glutathione is discussed.

Materials and methods

Cell cultivation

Cell cultures of canola (*Brassica napus*) purchased by DSMZ (Braunschweig, Germany) were grown in a modified Linsmaier and Skoog medium (http://www.dsmz.de/plant_cell_lines/medium/pdf/R.pdf). Cultures were maintained on a gyratory shaker (90 rpm) at 24°C in a 9-day growth cycle.

Incubation of cells with U

After 5 days of growth cell suspensions were filtered without suction through a nylon mesh of 50 µm pore size and resuspended in phosphate-free 50% fresh culture medium. Cell density was adjusted to 50 mg

fresh weight per liter). After 24 h incubation U was added from a 10⁻¹ M uranyl nitrate stock solution.

Assays of GSH/GSSH determination

Preparation of cell samples

All operations were done at 4°C. 10 ml cell suspension were taken at the indicated time points and subsequently drawn by a vacuum filtration unit (Sartorius, Göttingen, Germany). The supernatant was discarded whereas the cell pellet was immediately resuspended in 5 ml 100 mM KCl, 10 mM phosphatebuffer (pH 7.4). Cells were mechanically disrupted using a glass homogenizer. Cellular debris was separated from the soluble cell components by centrifugation at 13,000×g. Proteins were gently precipitated by acetone (final concentration 80%). The resulting supernatant was immediately concentrated to a final volume of 200 µl by rotary evaporation under vacuum conditions. Different tags of distinct functional groups were used for determination: (i) In case of GSH, the thiol functionality was tagged by monobromobimane (MBB; stock solution 10 g l⁻¹ in ethanol, final concentration 1 g l⁻¹) yielding a fluorescent product (Newton et al. 1981). The half diluted cytoplasmic extract was incubated 30 min with MBB in the dark. (ii) In case of GSSG the amino functionality was tagged by 2,4 dinitrobenzol (DNFB, Sanger reagent) (Sanger 1945) yielding a yellow coloured product (DNP-GSSG). Excess DNFB was removed by diethyl ether extraction. This procedure allows a direct measurement of GSSG without any additional reducing step.

Reversed phase HPLC of labelled GSH/GSSG

In order to determine specifically GSH in presence of other SH-containing cellular compounds such as cysteine and GSSG in the presence of many NH₂-containing metabolites, respectively, two separate chromatographic runs were performed.

5 µl of 1:10 diluted bimane or DNP labelled extract was injected by an autosampler on a Zorbax Eclipse XBD-C18 column with 5 µm particle size, 4.6 × 150 mm (Agilent Technologies, Böblingen, Germany). The 1200 Series Quaternary LC System consisted of quaternary pump, multiple wavelength and fluorescence detector (all Agilent Technologies). Elution was run with a gradient of 40–80% methanol

and 60–20% 0.01 mM phosphatebuffer, pH 6.0 within 10 min according to Zhang and Wong (1996). Detection of absorbing compound was realized at 340 nm whereas fluorescent compounds were detected at excitation 380 nm and emission 470 nm.

Calculation of cellular GSH/GSSG content

Chromatograms were analyzed by ChemStation software (Agilent Technologies). Calibration curves were established by using commercial available GSH and GSSG, respectively. The amounts were calculated by determining the “area under the curve” with baseline correction. With the reference to the cellular level, the cell count of samples was estimated (see below) and related to the measured concentration.

Estimation of the cell amount

The amount of cells in each sample was estimated using an averaged cell volume of $0.1 \times 10^{-4} \text{ mm}^3$. This is possible because of use of cell suspensions with relative equal cell shapes. To obtain the cell number, cells were visually counted on a Neubauer counting cell chamber using a fluorescence microscope (Axiovert, Carl Zeiss MicroImaging, Jena, Germany) and subsequently related to the sample volume of 10 ml.

Assay of cellular reducing capacity (MTT test)

Cellular reduction of C,N-diphenyl-N'-4,5-dimethylthiazol-2-yltetrazolium bromide (MTT) (Slater et al. 1963) was conducted by 3 h incubation of 500 μl cell suspensions with 100 μl MTT (stock solution 5 g l^{-1} in phosphate buffered saline) in the dark. After centrifugation at $13,000 \times g$, the purple formazan was extracted from the cell pellet with 500 μl acid isopropanol containing 0.04 M HCl. Extracted solutions were separated into 100 μl aliquots and the absorbance was subsequently measured in a 96-well microtiterplate in a microplate reader (Mithras LB 940, Berthold Technologies, Bad Wildbad, Germany) at 620 nm.

Artificial depletion of cellular GSH by chlorodinitrobenzene (CDNB)

The well-known inhibitor of GSH synthesis buthionine sulphoximine (BSO) (Earnshaw and Johnson

1985) failed to deplete the cellular GSH level (data not shown). Consequently, 1-chloro-2,4-dinitrobenzene (CDNB) was used to consume GSH (Mannervik and Danielson 1988). Cells were pre-incubated with 75 μM CDNB for 1 h, a further addition of the same concentration was made with U amendment.

In vitro reduction of U(VI) by GSH

All experimental steps were done under nitrogen atmosphere. 500 μM GSH and 100 μM uranyl nitrate were incubated by medium of ionic strength 0.1 M (sodium perchlorate) and pH 5.7 and 7.4, respectively. A 2 ml sample was taken after 24 h and acidified (pH < 1). This solution was extracted with 0.5 M 2-thenoyltrifluoroacetone (TTA) in vented xylol according to Bertrand and Chopin (1982) and Sachs and Bernhard (2011), respectively. Phase separation was done by centrifugation at $4,000 \times g$ 10 min. The non reduced U(VI) remains in the lower aqueous phase and was determined by inductively coupled plasma-mass spectrometry (ICP-MS; Elan 9000, Perkin Elmer, Waltham, USA) as previously described (Viehweger and Geipel 2010). The U(IV) amount was calculated using the measurement of the total initial U concentration by ICP-MS in the initial approach.

Photoacoustic determinations

Ten millilitre cell suspension were taken at the indicated time points and subsequently centrifuged at $13,000 \times g$ and therefore separated into outer and cellular medium, respectively. Sulfuric acid was added to the outer medium reaching a final concentration of 2 N. Soluble cellular compounds were extracted as described for the assays of GSH/GSSG determinations except acetone precipitation and concentration. The acidified extracts (final concentration of 2 N sulfuric acid) were centrifuged to remove precipitation (mainly cytoplasmic proteins). U(IV) was determined by laser-induced photoacoustic spectroscopy (LIPAS) according to Viehweger and Geipel (2010).

Statistical analysis

Calculated data were subjected to statistical analysis using GraphPadPrism version 5.02 for Windows (GraphPad Software, San Diego, USA). Investigations

of significant differences in GSH and GSSG concentrations and half cell reduction potentials, respectively, were carried out by two-way analysis-of-variance (ANOVA) followed by Bonferroni post-test (Figs. 1, 2). Significances between different time points were calculated using one-way analysis-of-variance (ANOVA) followed by Tukey's multiple comparison test (Fig. 2). Spectra (Fig. 3) were fitted with

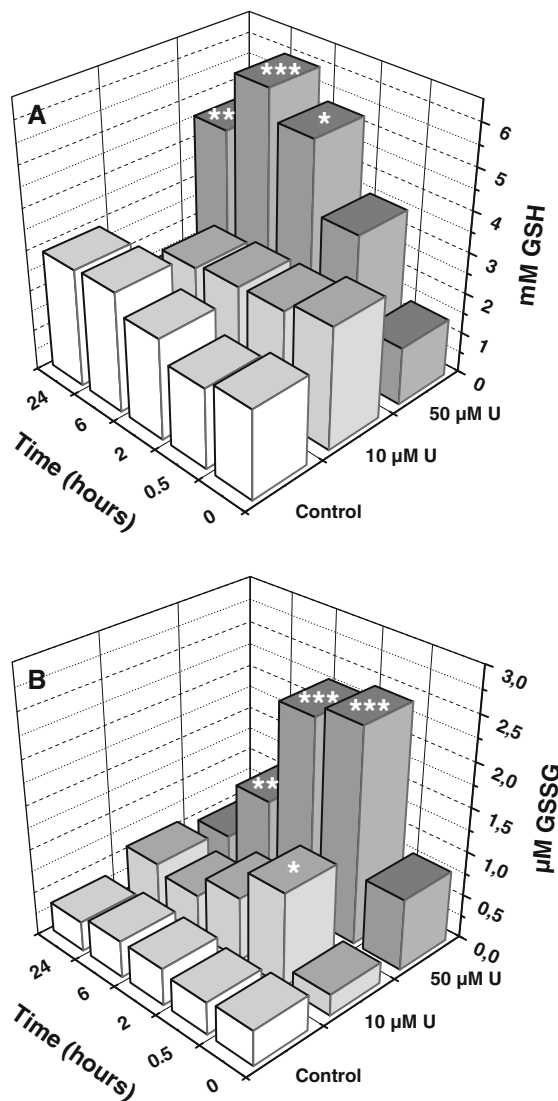


Fig. 1 Absolute concentrations of GSH (a) and GSSG (b) measured by HPLC. Data are means of 3 independent experiments for each U concentration, SD \pm 0.9 for GSH and SD \pm 0.3 for GSSG. Asterisks denote significant differences between controls and U treatments (two-way ANOVA; *** P < 0.001; ** P < 0.01; * P < 0.05)

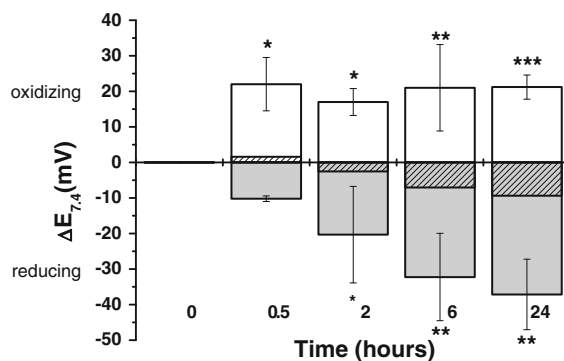


Fig. 2 Development of the half-cell reduction potential of 2GSH/GSSG calculated using Eq. 1 and the values from Fig. 2. Open columns represent addition of 10 μM U, filled columns 50 μM U and hatched columns the control. Data are means \pm SD of 3 independent experiments for each U concentration, SD \pm 3.2 mV for control. Asterisks denote significant differences between controls and U treatments (two-way ANOVA; *** P < 0.001; ** P < 0.01; * P < 0.05)

series of Gaussian peaks using GRAMS Spectroscopy Software Suite (Adept Scientific, Frankfurt/M, Germany).

Results

Effects of U on the cellular GSH/GSSG pool

The cellular GSH remained constant within the first 6 h of contact with 10 μM U (Fig. 1a). In contrast, 50 μM U induced a strong increase of GSH up to the 5 fold of the initial level (Fig. 1a).

The level of GSSG was raised up to 5 fold in the presence of U compared with the respective initial values (Fig. 1b). However, the starting level was reached after 24 h.

Glutathione redox potential in response to different U concentrations

The half-cell reduction potential of the couple 2GSH/GSSG can be calculated using an adapted Nernst equation (Eq. 1). Assuming a cytoplasmic pH of 7.4 and a temperature of 25°C, the commonly tabulated $E_{\text{pH} = 7.4} = -264$ mV (Rost and Rapoport 1964; Schafer and Buettner 2001) was used for calculations. This representative redox couple provides quantitative estimations of the redox state and can therefore

Fig. 3 Transient occurrence of U(IV) in the cytoplasm determined by LIPAS. *Upper part* shows an overview of typical absorption spectra obtained from prepared cellular matrices after contact with 10 μM U at indicated time points. *Lower part* shows the time response of LIPAS intensity representing U(IV). One typical sequence of spectra is shown from 3 independent experiments. Spectra were processed by Gaussian deconvolution

illustrate the cellular redox environment during U contact.

$$E = -267 \text{ mV} - (59.1/2)\log([\text{GSH}]_2/[\text{GSSG}]) \text{ mV} \times (25^\circ\text{C}, \text{pH } 7.4) \quad (1)$$

Additions of 10 μM U caused a shift of around 20 mV to a more oxidative environment (Fig. 2). In contrast, higher U concentrations (50 μM) shifted the redox potential up to 40 mV to more reducing conditions.

Impact of the GSH pool on the reducing capacity of cells challenged with U

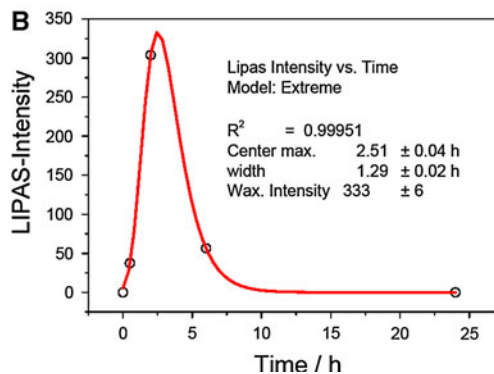
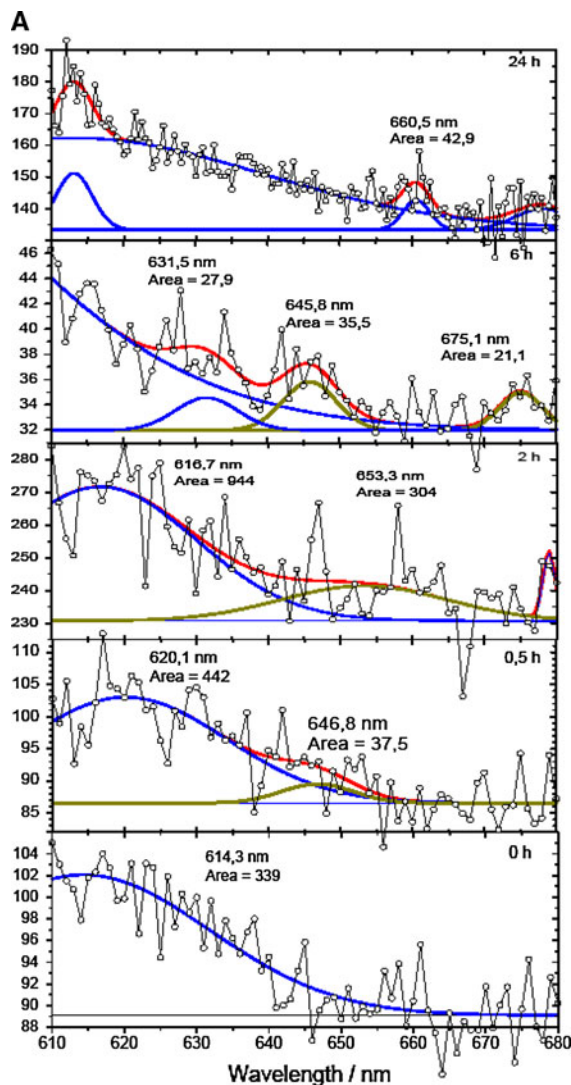
The cellular reducing capacity based on NAD(P)H detected by the reduction of MTT was not significantly impaired by U (Table 1). Only higher U concentrations (50 μM) caused a significant decrease during the first hour. However, artificial depletion of cellular GSH by chlorodinitrobenzene (CDNB) (70–80% decrease of the basic GSH level) induced a drastic increase of MTT reduction up to the double of the initial value.

Additional amendment of low U concentrations (10 μM) revealed only marginal changes of the highly reducing cellular conditions (Table 1). In contrast, higher U concentrations (50 μM) drastically decreased the reduction of MTT under GSH depletion.

In vitro reduction of U(VI)–U(IV) by GSH

The half-cell reduction potential of the GSH/GSSG couple at pH 7.4 and 25°C is –264 mV (reviewed in Schafer and Buettner 2001). Hence, the redox buffer provides a strong reducing capacity which should be able to reduce U(VI)–U(IV) keeping in mind the half-cell reduction potential of U(VI)/U(IV) of 0.3 mV.

67.5% ± 1.1 of the initial U(VI) content remained in this oxidation state after 24 h incubation with GSH at pH 5.8. The same amount (68.3% ± 0.4) could be



detected at pH 7.4. It should be noted that these values were obtained without additional electron donors or acceptors. The proton concentration has no

Table 1 Reducing activity of cells during different treatments in dependency of time

Time (hours)	10 μ M U	50 μ M U	75 μ M CDNB	75 μ M CDNB + 10 μ M U	75 μ M CDNB + 50 μ M U
1	117	63	195	189***	78
1.5	87	102	185	260***	54*
6	117	124	94	144**	41***

Each value represents the percentage portion (100% = initial activity) at the indicated time point. All values are means of 4 replicates, SD \sim 20%. Asterisks denote significant differences between the U treated cells and U + CDNB treated cells, respective (two-way ANOVA, *** $P < 0.001$; ** $P < 0.01$; * $P < 0.05$)

influence on the degree of the reduction within the pH range 5.6 and 7.4.

Occurrence of U(IV) in the cytoplasm

The absorption spectrum of U(IV) is characterized by typical maxima in the range of 630–680 nm (Viehweger and Geipel 2010). Figure 3 describes the occurrence of U(IV) in dependence of time in the cytoplasm after U(VI) addition to the culture medium. The U(IV) designated peak maxima showed an increasing intensity in the initial stage of cellular U contact (first 2 h) afterwards the intensity decreased (Fig. 3b). Almost no U(IV) could be detected after 24 h. Spectra of control cells displayed at most one peak maximum in the range of 660 nm as it is described at 0 and 24 h, respectively (Fig. 3a).

Discussion

The cellular GSH level remained relatively constant with 10 μ M U except a 50% decrease after 24 h (Fig. 1a). The reason for this is unclear. On the contrary, 50 μ M U caused a drastic increase of GSH. Such high U concentrations apparently induced the formation of ROS and free radicals. Recent studies revealed similar responses to U in *Arabidopsis thaliana* plants: Lower U concentrations (<100 μ M) induced no oxidative stress related responses whereas plants with higher U amounts suffered from oxidative stress (Vanhoudt 2009). As discussed before, U is a redox-active heavy metal which can directly generate

ROS via Fenton like reactions. The detoxification of ROS is GSH dependent and generates GSSG. Such a GSH consuming process and an excess of ROS activate GSH synthesis (reviewed in Foyer and Noctor 2005). A higher GSH level was also observed in primary leaves of U treated beans (*Phaseolus vulgaris*) (0.1–100 μ M U) (Vandenhove et al. 2006).

U triggered the accumulation of cellular GSSG (Fig. 1b) which often also led to subsequent increases of total glutathione (reviewed in Noctor 2006). These changes in glutathione status induced cellular redox imbalances. U treated plants (*Phaseolus vulgaris* and *Arabidopsis thaliana*) reacted on such disturbances with different antioxidant defense mechanisms such as increased capacities of antioxidative enzymes like peroxidases, increased transcript levels of NADPH oxidase and the occurrence of lipid peroxidation products (Vandenhove et al. 2006; Vanhoudt et al. 2008).

Another expression for these imbalances is the altered half-cell reduction potential of the couple 2GSH/GSSG. Moderate U concentrations (10 μ M) shifted the cellular redox environment towards more oxidizing conditions due to elevated GSSG levels whereas higher U concentrations (50 μ M) enhanced the reducing capacity of the cell (Fig. 2) due to a more pronounced increase of GSH. Such different defense reactions induced by lower and higher concentrations of biotic or abiotic stress are well known. For example, elevated pathogen attacks induced defense pathways including elements of hypersensitive response (Viehweger et al. 2006). Surprisingly, the redox potential was constantly elevated over the measured time (10 μ M U) so that it can not only act as a signal in antioxidant pathways. This indicates permanent redox cycles in the cell induced by U. The enhanced reducing capacity in the case of 50 μ M U can be attributed to an elicitation of hypersensitive response.

The reduction of MTT as an additional estimation of the reducing capacity of cells was not significantly impaired by 10 μ M U (Table 1, second column). This can be attributed to the fact that MTT reduction is mainly caused by NAD(P)H and partly by succinate dehydrogenases (Berridge and Tan 1993). In contrast, artificial depletion of cellular GSH by CDNB induced a significant (two-way-ANOVA, *** $P < 0.001$) strong increase of the reducing capacity (Table 1, fourth column). This result underlines the importance

of GSH in cellular redox homeostasis because of an obvious enhancement of metabolic processes during depletion of GSH. The significant “overproduction” of reducing agents caused by lack of GSH and simultaneous presence of low U concentrations describes the efforts of cells to overcome this stress situation (Table 1, fifth column). Concerning higher U concentrations, there was a slight but significant decrease in the initial phase of U contact which indicates a consumption of cellular reducing agents (Table 1, third column). U contact under low GSH levels induced an obvious break down of antioxidative defense mechanisms suggested by a significant loss of cellular reducing capacity (Table 1, sixth column). The results suggest that the cellular GSH content is inversely linked to U sensitivity and underlines the important role of GSH in avoiding heavy metal toxicity (reviewed, e.g., in Sharma and Dietz 2009).

An additional element of U detoxification mechanisms is the complex formation between the heavy metal and GSH. Recent studies on UO_2^{2+} and GSH suggest the metal coordination at the two carboxylic functionalities of GSH forming a cyclic complex (Frost et al. 2011). The redox sensitivity of the sulfhydryl moiety was blocked by different compounds in these experiments. However, the free thiol moiety is oxidation sensitive building a disulfide bridge between two GSH molecules. GSH was able to reduce U(VI)–U(IV) up to a value of 33% reduced U in vitro. Since one GSH molecule releases one electron and two molecules are necessary for forming the oxidized dimer it is possible that each GSH bears a uranyl ion at the carboxylic functionalities and one electron is transferred to each uranyl forming UO_2^+ . This oxidation state subsequently disproportionates to UO_2^{2+} and U^{4+} . The latter will probably be released from the GSSG. Excess GSH should preferentially coordinate U^{4+} at the sulfhydryl moiety as it was postulated for cysteine a component of GSH (Nazir and Naqvi 2010) whereas UO_2^{2+} binds at the carboxylic residues (Günther et al. 2007). Another hint for this coordination is the formation of phytochelatin after U contact (data not shown) which requires an occupied SH moiety (Vatamaniuk et al. 2000).

In vivo experiments proved a transient occurrence of U(IV) in the cytoplasm (Fig. 3). It is well known that U(IV) is less soluble than U(VI) in most cases. However, some soluble U(IV) compounds are known, for example with citrate (Francis and Dodge 2008), as

UO_2 nanoparticle (Ulrich et al. 2008) or as GSH complex (data not shown). Therefore, this U reduction can be a part of defense mechanism including complex formation with GSH and subsequent phytochelatin synthesis. The high stability constant of $\log\beta$ 38.65 of the GSH–U(VI) complex (Frost et al. 2011) and the ligand concentration in mM-range underline this. However, it can not be ruled out that metals of metalloproteins are substituted by a particular amount of U and might probably influence cellular electron transfer reactions due to its properties as transition metal. The additional absorption peaks (around 660 nm) in the photoacoustic determinations (Fig. 3) can be assigned to charge-transfer complexes between flavin adenine dinucleotide (FAD) and pyridine nucleotide (NADPH) (Massey and Ghisla 1974). These redox elements are crucial parts of enzymes belonging to the oxidoreductase family. Recent studies of the cytoplasmic metalloproteome of the microorganism *Pyrococcus furiosus* revealed a U containing ferritin (Cvetkovic et al. 2010). Ferritin as a known iron-protein belongs to the family of oxidoreductases.

Conclusions

The cellular redox balance in suspension cells of canola was impaired by contact with U. Lower U concentrations (10 μM) partly consumed the cellular reducing capacity thereby shifting redox potential to more oxidizing conditions. In contrast, higher U concentrations induced a more reducing cellular environment (higher GSH/GSSG ratios) indicating strong oxidative stress reactions. Two different, U concentration dependent defense pathways can be postulated: a specific after contact with lower U concentrations and an unspecific induced by higher concentrations, respectively. An additional element of defense includes complex formations between U and glutathione and a transient reduction of U(VI)–U(IV).

Acknowledgments We thank U. Schaefer, A. Ritter for ICP-MS measurements.

References

- Berridge MV, Tan AS (1993) Characterization of the cellular reduction of 3-(4, 5-dimethylthiazol-2-yl)-2, 5-diphenyltetrazolium bromide (MTT)-subcellular-localization, substrate

- dependence, and involvement of mitochondrial electron-transport in MTT reduction. *Arch Biochem Biophys* 303:474–482
- Bertrand PA, Choppin GR (1982) Separation of actinides in different oxidation-states by solvent extraction. *Radiochim Acta* 31:135–137
- Canovas D, Vooijs R, Schat H, de Lorenzo V (2004) The role of thiol species in the hypertolerance of *Aspergillus* sp. P37 to arsenic. *J Biol Chem* 279:51234–51240
- Cvetkovic A, Menon AL, Thorgersen MP, Scott JW, Poole FL, Jenney FE, Lancaster WA, Praissman JL, Shanmukh S, Vaccaro BJ, Trauger SA, Kalisiak E, Apon JV, Siuzdak G, Yannone SM, Tainer JA, Adams MWW (2010) Microbial metalloproteomes are largely uncharacterized. *Nature* 466:718–779
- Earnshaw BA, Johnson MA (1985) The effect of glutathione on development in wild carrot suspension-cultures. *Biochem Biophys Res Commun* 133:988–993
- Foyer CH, Noctor G (2005) Redox homeostasis and antioxidant signaling: a metabolic interface between stress perception and physiological responses. *Plant Cell* 17:1866–1875
- Frost L, Geipel G, Viehweger K, Bernhard G (2011) Interaction of uranium(VI) towards glutathione: an example to study different functional groups in one molecule. *Radiochim Acta* (in press)
- Günther A, Bernhard G, Geipel G, Reich T, Rossberg A, Nitsche H (2003) Uranium speciation in plants. *Radiochim Acta* 91:319–328
- Günther A, Geipel G, Bernhard G (2007) Complex formation of uranium(VI) with the amino acids L-glycine and L-cysteine: a fluorescence emission and UV-Vis absorption study. *Polyhedron* 26:59–65
- Mannervik B, Danielson UH (1988) Glutathione transferases: structure and catalytic activity. *Crc Crit Rev Biochem* 23:283–337
- Massey V, Ghisla S (1974) Role of charge-transfer interactions in flavoprotein catalysis. *Ann NY Acad Sci* 227:446–465
- Nazir M, Naqvi II (2010) Synthesis and characterization of uranium (IV) complexes with various amino acids. *J Saudi Chem Soc* 14:101–104
- Newton GL, Dorian R, Fahey RC (1981) Analysis of biological thiols: derivatization with monobromobimane and separation by reverse-phase high-performance liquid chromatography. *Anal Biochem* 114:383–387
- Noctor G (2006) Metabolic signalling in defence and stress: the central roles of soluble redox couples. *Plant Cell Environ* 29:409–425
- Noctor G, Foyer CH (1998) ASCORBATE AND GLUTATHIONE: keeping active oxygen under control. *Ann Rev Plant Physiol Plant Mol Biol* 49:249–279
- Rost J, Rapoport S (1964) Reduction-potential of glutathione. *Nature* 201:185
- Sachs S, Bernhard G (2011) Humic acid model substances with pronounced redox functionality for the study of environmentally relevant interaction processes of metal ions in the presence of humic acid. *Geoderma* 162:132–140
- Sanger F (1945) The free amino groups of insulin. *Biochem J* 39:507–515
- Schafer FQ, Buettner GR (2001) Redox environment of the cell as viewed through the redox state of the glutathione disulfide/glutathione couple. *Free Radic Biol Med* 30:1191–1212
- Sharma SS, Dietz KJ (2009) The relationship between metal toxicity and cellular redox imbalance. *Trends Plant Sci* 14:43–50
- Singh BK (2005) Complexation behaviour of glutathione with metal ions. *Asian J Chem* 17:1–32
- Slater TF, Sawyer B, Strauli U (1963) Studies on succinate-tetrazolium reductase systems 3. Points of coupling of 4 different tetrazolium salts. *Biochim Biophys Acta* 77:383–393
- Ulrich KU, Singh A, Schofield EJ, Bargar JR, Veeramani H, Sharp JO, Bernier-Latmani R, Giammar DE (2008) Dissolution of biogenic and synthetic UO₂ under varied reducing conditions. *Environ Sci Technol* 42:5600–5606
- Vandenhove H, Cuypers A, Van Hees M, Koppen G, Wannijn J (2006) Oxidative stress reactions induced in beans (*Phaseolus vulgaris*) following exposure to uranium. *Plant Physiol Biochem* 44:795–805
- Vanhoudt N (2009) Study of biological effects induced in *Arabidopsis thaliana* following uranium exposure, including mixed exposure to cadmium or external gamma radiation: applying a multi-biomarkers approach. Thesis, Hasselt University Diepenbeek, Belgium
- Vanhoudt N, Vandenhove H, Smeets K, Remans T, Van Hees M, Wannijn J, Vangronsveld J, Cuypers A (2008) Effects of uranium and phosphate concentrations on oxidative stress related responses induced in *Arabidopsis thaliana*. *Plant Physiol Biochem* 46:987–996
- Vatamaniuk OK, Mari S, Lu YP, Rea PA (2000) Mechanism of heavy metal ion activation of phytochelatin (PC) synthase: blocked thiols are sufficient for PC synthase-catalyzed transpeptidation of glutathione and related thiol peptides. *J Biol Chem* 275:31451–31459
- Viehweger K, Geipel G (2010) Uranium accumulation and tolerance in *Arabidopsis halleri* under native versus hydroponic conditions. *Environ Exp Bot* 69:39–46
- Viehweger K, Schwartze W, Schumann B, Lein W, Roos W (2006) The G alpha protein controls a pH-dependent signal path to the induction of phytoalexin biosynthesis in *Eschscholzia californica*. *Plant Cell* 18:1510–1523
- Zhang K, Wong KP (1996) Inhibition of the efflux of glutathione S-conjugates by plant polyphenols. *Biochem Pharmacol* 52:1631–1638